

# Global Average Potassium Isotope Composition of Modern Seawater

Kun Wang,\* Hilary G. Close, Brenna Tuller-Ross, and Heng Chen

Cite This: *ACS Earth Space Chem.* 2020, 4, 1010–1017

Read Online

ACCESS |



Metrics &amp; More



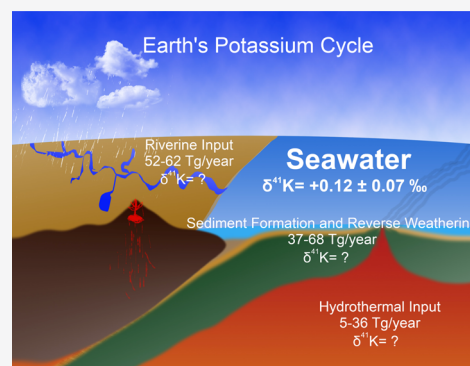
Article Recommendations



Supporting Information

**ABSTRACT:** The potassium isotope system was proposed as a new tracer in continental weathering and global K cycling. The largest K isotope fractionation observed among major reservoirs is between the ocean and bulk silicate Earth (BSE). Seawater is significantly enriched in heavy isotopes compared to BSE, and seawater represents the heaviest reservoir on Earth. Because of limited analyses, it is still unknown whether seawater is homogeneous in terms of K isotopes vertically, laterally, and globally. In addition, what processes (e.g., hydrothermal inputs) and to what degrees these processes have contributed to this heavy isotope enrichment in seawater are still not well constrained. To better understand the K isotopic compositions of modern seawater and to examine the possible influence of seafloor hydrothermal vents on the K isotope composition of seawater, we analyzed the K isotope composition of 46 seawater samples collected as two pairs of depth profiles in two locations from the Atlantic and Pacific oceans, including one near an active hydrothermal vent field (ASHES, Axial Seamount, Juan de Fuca Ridge). We found that within the current analytical uncertainty, all seawater samples have the same K isotope composition regardless of their location, depth, [K] concentration, and salinity. Combining our new analyses with data from previous studies, we define the best representative K isotope composition of modern seawater as  $+0.12 \pm 0.07\text{‰}$  (2SD). The seawater is significantly higher ( $0.55 \pm 0.18\text{‰}$ ) than BSE, which requires large K isotopic fractionation during continental weathering and reverse weathering.

**KEYWORDS:** potassium isotopes, ASHES vent field, Juan de Fuca Ridge, hydrothermal fluids, average seawater composition



## 1. INTRODUCTION

Understanding modern ocean chemistry and reconstructing the evolution of ocean chemistry over geologic time are imperative to understanding Earth's evolution into a habitable planet. Previous studies have shown that chemical exchange between the lithosphere and hydrosphere is a key process in regulating a steady-state ocean composition.<sup>1–5</sup> Potassium (K) is a major component of both lithosphere and hydrosphere (2.8% K<sub>2</sub>O in continental crust; 0.11% K<sub>2</sub>O in oceanic crust; and 399 ppm K in seawater),<sup>6–8</sup> and accordingly, potassium isotopes have been recently proposed as a potential tracer for understanding the K budget in seawater and K exchange between the lithosphere and hydrosphere.<sup>3,9,10</sup> Since 2016, with improved precision in analyzing K isotopes using multicollector inductively coupled plasma mass spectrometers (MC-ICP-MSs),<sup>11–15</sup> it has been consistently shown that seawater is enriched in heavier isotopes compared to the bulk silicate Earth (BSE); however, the mechanism of enrichment is still not well understood.<sup>9</sup>

Potassium is a major cation in seawater, and its residence time ( $\tau$ ) is  $\sim 11$  million years.<sup>16</sup> The two major inputs of K in seawater are riverine and hydrothermal. The flux of K from riverine inputs is relatively well constrained, ranging from 52 to 62 Tg/year,<sup>17–19</sup> and the K isotope compositions of dissolved

K in rivers vary from  $-0.44$  to  $+0.12\text{‰}$  (averaging at  $-0.22\text{‰}$ ).<sup>9</sup> The hydrothermal flux is less constrained, ranging from 5 to 36 Tg/year,<sup>1,5,17–20</sup> and there is no publication yet that reports direct measurements of K isotopic compositions of hydrothermal fluids.<sup>21</sup> To balance the K budget in seawater, one must consider the two major processes for removing K ions from seawater: marine sediment formation and low-temperature alteration of basalts. The flux of K incorporated into sediments is estimated to be 25 to 52 Tg/year,<sup>1,17,18</sup> and the K isotope fractionation factor between sediments and seawater ( $\Delta_{\text{sediment-seawater}}$ ) during authigenic clay formation is inferred to be  $-2$  to  $0\text{‰}$ .<sup>22</sup> The flux of K incorporated into low-temperature altered basalts is 12 to 15.6 Tg/year,<sup>17,18</sup> and the K isotope fractionation factor between low-temperature altered oceanic crust (AOC) and seawater ( $\Delta_{\text{AOC-seawater}}$ ) is estimated to be  $\sim 0\text{‰}$ .<sup>3</sup> As previously demonstrated,<sup>9</sup> K isotopes can be used to better constrain the fluxes of different

Received: February 15, 2020

Revised: June 18, 2020

Accepted: June 19, 2020

Published: June 19, 2020

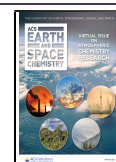


Table 1. K Concentration and Isotopic Compositions of Atlantic and Pacific Seawater Profiles

sample	latitude	longitude	depth [m]	K [ppm]	$\delta^{41}\text{K}$ [‰] 2SD	<i>n</i>
Atlantic Seawater						
cast 3-3	25.50814	-79.863				
C3-3-A			352	400	0.10 ± 0.13	10
C3-3-B			147	415	0.08 ± 0.21	10
C3-3-C			95	408	0.10 ± 0.16	10
C3-3-D			71	412	0.13 ± 0.20	10
C3-3-E			57	408	0.14 ± 0.10	10
C3-3-F			22	411	0.12 ± 0.16	10
				average=	0.11 ± 0.04	
cast 3-4	25.54231	-79.845				
C3-4-1			692	396	0.19 ± 0.19	10
C3-4-2			526	388	0.10 ± 0.16	10
C3-4-3			450	397	0.16 ± 0.14	10
C3-4-5			284	400	0.14 ± 0.05	10
C3-4-6			214	417	0.14 ± 0.05	10
C3-4-7			180	417	0.12 ± 0.06	10
C3-4-8			110	412	0.11 ± 0.07	10
C3-4-9			80	405	0.14 ± 0.07	10
C3-4-10			51	415	0.16 ± 0.13	10
C3-4-11			31	406	0.13 ± 0.03	10
C3-4-12			5	411	0.15 ± 0.04	5
				average=	0.14 ± 0.05	
				Atlantic average=	0.13 ± 0.05	
Pacific Seawater						
station 17	45.941	-130.019				
17-1-1			1537	297	0.02 ± 0.13	10
17-1-2			1482	308	-0.01 ± 0.13	11
17-1-3			1285	354	0.08 ± 0.16	11
17-1-4			1088	346	0.08 ± 0.13	12
17-1-5			891	354	0.02 ± 0.12	11
17-1-6			693	354	0.04 ± 0.11	11
17-1-7			495	369	0.09 ± 0.12	11
17-1-8			396	431	0.03 ± 0.12	11
17-1-9			297	348	0.02 ± 0.11	10
17-1-10			198	354	0.11 ± 0.12	10
17-1-11			149	354	0.07 ± 0.08	12
17-1-12			99	341	0.11 ± 0.09	12
17-1-13			65	358	0.13 ± 0.10	12
17-1-14			45	389	0.07 ± 0.11	12
17-1-15			10	349	0.12 ± 0.11	12
				average=	0.07 ± 0.09	
station 18	45.829	-129.452				
18-2-1			1509	307	0.05 ± 0.08	12
18-2-2			1384	346	0.06 ± 0.09	12
18-2-3			1187	367	0.12 ± 0.12	12
18-2-4			990	390	0.11 ± 0.19	10
18-2-5			792	384	0.07 ± 0.14	10
18-2-6			594	357	0.08 ± 0.12	12
18-2-7			396	375	0.08 ± 0.14	12
18-2-8			297	367	0.08 ± 0.14	12
18-2-9			198	370	0.10 ± 0.13	12
18-2-10			149	351	0.09 ± 0.10	12
18-2-11			99	360	0.05 ± 0.17	12
18-2-12			55	362	0.09 ± 0.17	12
18-2-13			35	378	0.09 ± 0.08	12
18-2-14			10	360	0.12 ± 0.09	12
				average=	0.09 ± 0.05	
				Pacific average=	0.07 ± 0.07	
				grand average=	0.10 ± 0.08	

inputs and outputs and to improve our understanding of the modern K cycle. However, because of the as-of-yet limited availability of high-precision K isotope data for seawater, river water, hydrothermal fluids, marine sediments, and altered oceanic basalts, it is still challenging to achieve the full potential of applying K isotopes into such mass-balance calculations.<sup>9</sup>

Even the global K isotope composition of modern seawater is not well defined. There are four reports of K isotope data for seawater: (i) one Pacific seawater sample (TPS 24°N, station 35, 400 m), which is  $0.10 \pm 0.07\text{‰}$  (2SE);<sup>11</sup> (ii) one Atlantic seawater sample (IAPSO standard seawater purchased from OSIL) from an unknown location in the open Atlantic ocean, which is  $0.06 \pm 0.03\text{‰}$ ;<sup>12</sup> (iii) one Atlantic seawater sample from Bermuda at  $0.03 \pm 0.03\text{‰}$ <sup>13</sup> (note: this value was converted from their reported value via SRM 999b); and (iv) one Pacific seawater sample from Hawaii reported by the University of Washington,<sup>14,23</sup> which is  $0.14 \pm 0.01\text{‰}$ . Although these four seawater samples (two from the Pacific and two from the Atlantic) have similar K isotopic compositions within analytical errors, the range spans from 0.03 to 0.14‰. Whether this 0.11‰ variation is simply due to interlaboratory analytical uncertainties<sup>15</sup> or represents real heterogeneity is still unknown. Considering that the entire range of K isotopic variation among all terrestrial samples is typically less than  $\sim 2\text{‰}$ ,<sup>11–14</sup> it is crucial that the global K isotope composition of seawater be better determined before the K isotope system can be applied as a tracer in studies of continental weathering and global K cycling. Until recently,<sup>24</sup> there has been no systematic study on K isotopic variation among samples from different locations and from various depths. In addition, there is no evaluation yet of the influence of seafloor hydrothermal vent plumes on the K isotope homogeneity of seawater.

Here, we present new high-precision measurements of the K isotope compositions of 46 seawater samples from two pairs of water columns in both the Atlantic and Pacific oceans. Among them, two water columns are near the hydrothermal vent field, where the presence of plume influence is expected. The purpose of this study is two-fold: first, to evaluate the homogeneity of K isotopes in seawater from varying locations and at varying depths, as well as the influence of hydrothermal K on the homogeneity of K isotopes in seawater; second, to determine the best available estimate of the K isotope composition of modern seawater using results from this study and previously published data.

## 2. SAMPLES AND METHODS

**2.1. Sample Description.** A total of 46 individual samples analyzed in this study were collected from two pairs of seawater profiles in the Atlantic and Pacific oceans. All samples were whole seawater collected directly from a rosette of Niskin bottles into cryovials that were prerinsed with sample seawater and stored at  $-20\text{ °C}$ . The sample numbers and locations are listed in Table 1.

Atlantic samples ( $n = 17$ ) were collected on April 20, 2019 on R/V F.G. Walton Smith (Cruise ID: WS19110). The samples were obtained from two locations, cast 3–3 and cast 3–4, which were approximately 4.3 km apart. At location 3–3 ( $n = 6$ ), sample depths ranged from 22 to 352 m below the surface. At location 3–4 ( $n = 11$ ), depths ranged from 5 to 692 m below the surface.

Pacific samples ( $n = 29$ ) were collected on August 20 and 21, 2018 on R/V oceanus (Cruise ID: OC1808C). The samples were obtained from two locations: station 17 ( $n = 15$ ) and station 18 ( $n = 14$ ). Station 17 and station 18 are directly above the Axial Seamount Hydrothermal Emission Study (ASHES) vent field (100 m by 90 m; depth 1542 m) in the Axial Volcano of the Juan de Fuca Ridge.<sup>25,26</sup> Two more active hydrothermal vent systems in Axial Volcano are located within close distance: Canadian American Seamount Expedition (8 km north) and the International District (3 km east). Axial Volcano is the most active volcano on the Juan de Fuca Ridge.<sup>27</sup> At both, stations 17 and 18, samples were collected at varying depths between 10 and  $\sim 1550$  m below the sea surface, the deepest being within 70 m from the sea floor.

**2.2. Analytical Method.** The analytical method used in this study is reported in greater detail in ref 15. Other groups<sup>11–14</sup> have reported the use of similar methods, and cross-laboratory comparisons of K isotopes measured in geostandards have shown that the methods of these groups produce data that generally agree with each other within the current limits of analytical uncertainty.<sup>15</sup> Our seawater samples were prepared and analyzed in four steps: (1) evaporation, digestion, and rehydration in acid; (2) purification for K using ion-exchange chromatography; (3) iCapQ quadrupole ICP–MS concentration and matrix analysis; and (4) isotope analysis with the Neptune Plus MC–ICP–MS.

**2.2.1. Sample Evaporation, Digestion, and Rehydration.** Between 3 and 5 mL of each sample was separated and frozen. Upon their arrival at Washington University in St. Louis, samples were allowed to thaw at room temperature and then weighed into Teflon beakers to ensure accurate records of their volumes. The samples were then left to evaporate under a heat lamp for several hours. Once evaporated, between 1 and 2 mL of concentrated nitric acid was added to each beaker before they were closed and heated overnight to sterilize the residual of any potential microbial material. The samples were then evaporated a final time and rehydrated in 5 mL of 2% nitric acid. There were no residual salts observed after rehydration. A 0.1 mL aliquot of the rehydrated, unpurified solution for each sample was then run through the iCapQ quadrupole ICP–MS to determine major element concentrations for the unpurified seawater. The remaining 4.9 mL of each sample was retained to be purified for K.

**2.2.2. Ion-Exchange Chromatography.** The ion-exchange chromatography method used to purify each sample for K was first proposed in 1970<sup>28</sup> and is extensively used in recent studies of potassium isotopes.<sup>11–15</sup> For each seawater sample, 0.5 mL of the rehydrated sample was passed through one cycle of “big” columns (filled with 17 mL BioRad AG50-X8 100–200 mesh cation-exchange resin) eluted with 0.7 N HNO<sub>3</sub>, and the resultant 111 mL collected solution, or “K-cut”, was evaporated under heat lamps. The residual was then rehydrated in 1 mL 0.5 N HNO<sub>3</sub> and passed through one cycle of “small” columns (filled with 2.4 mL of the same BioRad AG50-X8 100–200 mesh cation-exchange resin) eluted with 0.5 N HNO<sub>3</sub> to produce a 21 mL K-cut. This final K-cut was then evaporated under heat lamps and rehydrated in 5 mL of a 2% HNO<sub>3</sub> solution for analysis.

Prior to introducing the samples, columns were first rinsed with 60 or 14 mL 6 N HCl for big or small columns, respectively. Additionally, several milliliters (5 for big columns and 2 for small columns) were collected immediately before and after the K-cut volume, which serve as “precuts” and

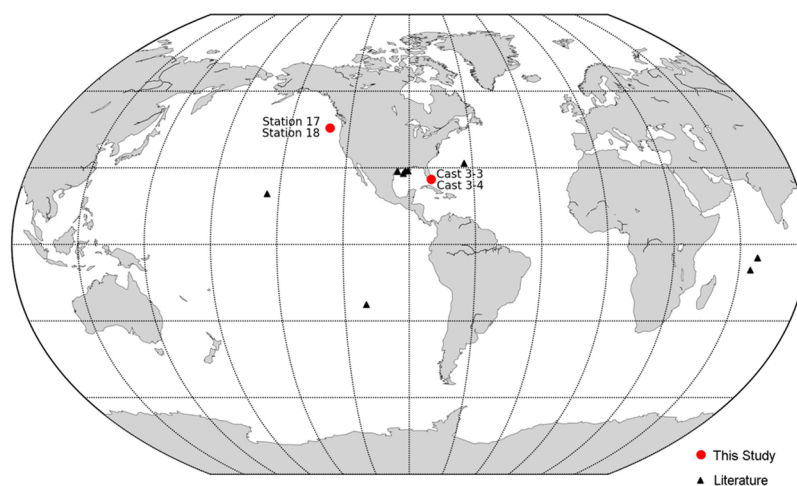


**Figure 1.** Sample location from this study (Pacific ocean: station 17 and 18; Atlantic ocean: cast 3–3 and 3–4) and literature.<sup>11–14,23,24</sup>

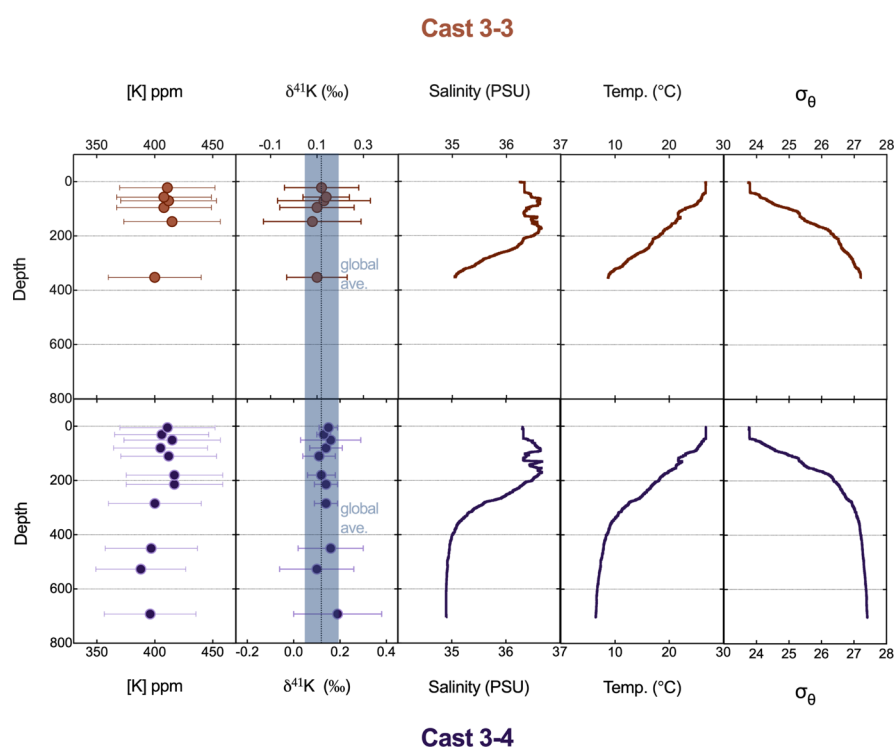


**Figure 2.** [K] abundance, K isotope composition, salinity, temperature, and potential density anomaly ( $\sigma_\theta$ ) vs sample depth at cast 3–3 and 3–4 from Atlantic ocean. The global average K isotope composition of seawater ( $+0.12 \pm 0.07\text{‰}$ ) is also plotted for comparison.

“postcuts” to compare with the K-cut. Chromatography steps and specifications are outlined in greater detail in the literature.<sup>15</sup>

**2.2.3. Elemental Analysis with iCapQ ICP–MS.** The aliquot of raw seawater and purified K-cut for each sample, along with their precuts and postcuts from both big and small columns, were analyzed against a multielement standard using the iCapQ quadrupole ICP–MS (Thermo Scientific, Bremen, Germany) in the Department of Earth and Planetary Sciences at Washington University in St. Louis. This serves two purposes: first, to ascertain whether any matrix elements remained in the solution for analysis, and second, to ensure complete (>99%) recovery of K. If any other element is found in the K-cut in amounts >1% relative to K, the sample is run through an additional cycle of small columns to avoid matrix

effects; this did not occur in any of our 46 analyzed samples because K is a major ion in seawater. The K concentrations acquired from iCapQ analysis were then used to dilute each sample to match our K standard (500 ppb NIST SRM3141a) within 3%.

**2.2.4. Isotopic Analysis Using MC–ICP–MS.** The diluted solutions were then analyzed in the Neptune Plus MC–ICP–MS (Thermo Scientific, Bremen, Germany) in the Department of Earth and Planetary Sciences at Washington University in St. Louis. Each sample was measured ~10 times using the standard-sample bracketing method. The average of the ~10 measurements is reported as each sample’s  $\delta^{41}\text{K}$  value, where  $\delta^{41}\text{K} = [({}^{41}\text{K}/{}^{39}\text{K})_{\text{sample}}/({}^{41}\text{K}/{}^{39}\text{K})_{\text{NIST SRM3141a}} - 1] \times 1000$  in units of per mille (‰). Analytical uncertainties are reported as 2 standard deviations (2SD), which are given for each sample

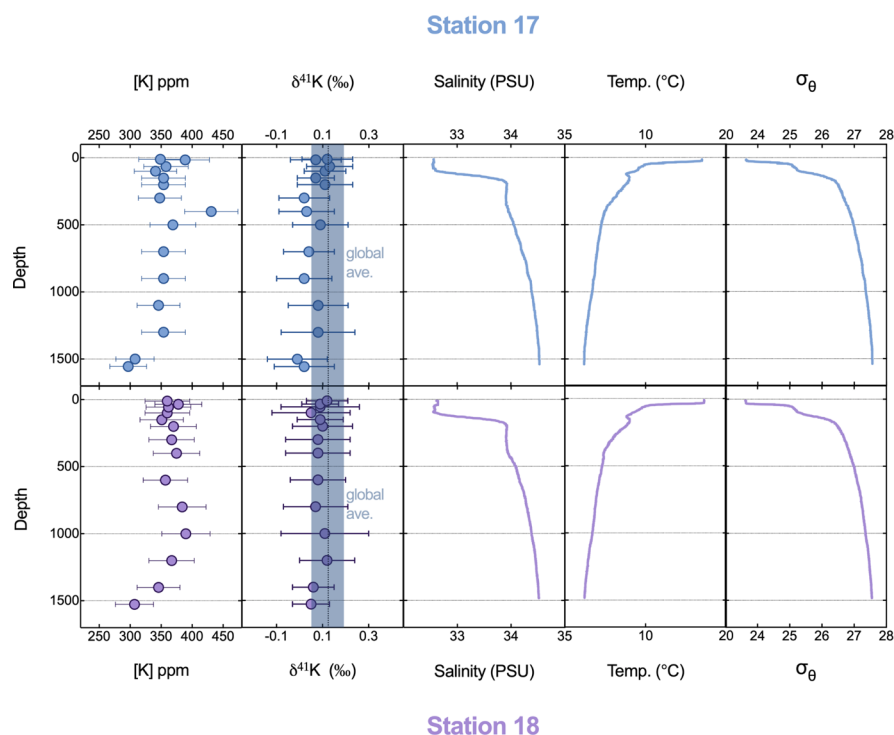


**Figure 3.** [K] abundance, K isotope composition, salinity, temperature, and potential density anomaly ( $\sigma_\theta$ ) vs sample depth at station 17 and 18 from Pacific ocean. The global average K isotope composition of seawater ( $+0.12 \pm 0.07\text{‰}$ ) is also plotted for comparison.

in Table 1. The long-term (20 months) reproducibility is  $\sim 0.11\text{‰}$  (2SD;  $n = 890$ ), and the total procedure blank is  $0.26 \pm 0.15 \mu\text{g}$  (2SD;  $n = 7$ ), which is negligible.<sup>15</sup>

### 3. RESULTS

Table 1 presents all the K concentrations and K isotope compositions of all four water columns analyzed in this study. Figure 1 shows the locations for all samples in this study as well as other seawater samples from the literature.<sup>11,13,14,23,24</sup> Figure 2 and 3 illustrate the K concentration, K isotope composition, salinity, temperature, and potential density anomaly ( $\sigma_\theta$ ) versus sample depth.

**3.1. Two Water Columns from Atlantic Ocean.** The six water samples from cast 3–3 (from 22 to 352 m water depth) have K concentrations varying from 400 to 415 ppm (average:  $409 \pm 10$  ppm) and K isotope compositions varying from  $0.08 \pm 0.21$  to  $0.14 \pm 0.10\text{‰}$  (average:  $0.11 \pm 0.04\text{‰}$ ). The 11 water samples from cast 3–4 (from 5 to 692 m water depth) have K concentrations varying from 388 to 417 ppm (average:  $406 \pm 19$  ppm) and K isotope compositions varying from  $0.10 \pm 0.16$  to  $0.19 \pm 0.19\text{‰}$  (average:  $0.14 \pm 0.05\text{‰}$ ). For each profile, there was no systematic variation in the K concentration and K isotope composition with sample depth. All Atlantic ocean samples have the same K isotope compositions within uncertainty. The grand average of K isotope compositions for all Atlantic ocean samples in this study is  $0.13 \pm 0.05\text{‰}$  (2SD), which agrees well with the Atlantic ocean average ( $0.14 \pm 0.02\text{‰}$ ) reported in literature.<sup>24</sup>

**3.2. Two Water Columns from Pacific Ocean Adjacent to Hydrothermal Vents.** The 15 water samples from station 17 (from 10 to 1537 m water depth) have K concentrations varying from 297 to 431 ppm (average:  $354 \pm 61$  ppm) and K isotope compositions varying from  $-0.01 \pm 0.13$  to  $0.13 \pm$

$0.10\text{‰}$  (average:  $0.07 \pm 0.09\text{‰}$ ). The 14 water samples from station 18 (from 10 to 1509 m water depth) have K concentrations varying from 307 to 390 ppm (average:  $362 \pm 40$  ppm) and K isotope compositions varying from  $0.05 \pm 0.08$  to  $0.12 \pm 0.09\text{‰}$  (average:  $0.09 \pm 0.05\text{‰}$ ). For each profile, there was no systematic variation in the K concentration and K isotope composition with sample depth. All Pacific ocean samples have the same K isotope compositions within uncertainty. The grand average of K isotope compositions for all Pacific ocean samples in this study is  $0.07 \pm 0.07\text{‰}$  (2SD), which is not significantly different from the average value of all Atlantic ocean samples ( $0.13 \pm 0.05\text{‰}$ ).

### 4. DISCUSSION

**4.1. Hydrothermal Influence on K Isotopic Heterogeneity of Seawater.** A main goal of this study is to constrain the hydrothermal input on the K isotope composition of seawater. In order to do so, we compare two water columns from the Atlantic, which are without any close affinity to a hydrothermal vent system, with the two water columns from the Pacific ocean (station 17 and 18) that are right above the ASHES vent field, Axial Seamount, Juan de Fuca Ridge. As shown previously,<sup>24</sup> there is no measurable difference in K isotopes between the Atlantic and Pacific open-ocean samples that are not adjacent to any hydrothermal vents. Thus, if we were to observe any difference between the two columns from the Atlantic and Pacific ocean samples in this study, the difference would likely be due to the hydrothermal influence from the ASHES vent field, an active hydrothermal system.<sup>25,26</sup>

Overall, the two pairs of depth profiles from both the Atlantic and Pacific ocean samples show variability in K isotope compositions to some degree. Particularly, the two

water columns right above the ASHES vent field show slightly higher variability than the two water columns not adjacent to any hydrothermal systems (2SD: 0.07 vs 0.05‰). However, neither water column shows statistically significant variation across its depth profile regardless of the distance to the hydrothermal vent (see Figures 2 and 3). We could reach this conclusion by comparing Pacific water samples from above and below the pycnocline (~200 m). In the mid-latitude Pacific, high rates of precipitation and/or advected freshwater mixing at the ocean surface create a strong halocline and pycnocline (Figure 3), which prevents mixing between waters above and below ~200 m. As a result, seawater chemical signatures originating at the seafloor are unlikely to reach depths shallower than 200 m. The upper 200 m of both water columns appear to have K isotope compositions that are indistinguishable from the subpycnocline waters:  $0.10 \pm 0.05$  vs  $0.04 \pm 0.07$ ‰ and  $0.09 \pm 0.05$  vs  $0.08 \pm 0.05$ ‰ for station 17 and 18, respectively.

When dissecting the data in more detail, it is intriguing to note that the deepest two samples in each column near the ASHES vent field display the lowest values ( $0.02 \pm 0.13$ ,  $-0.01 \pm 0.13$ ,  $0.05 \pm 0.08$ , and  $0.06 \pm 0.09$ ‰) among each column and the largest deviations from the global average ( $0.10 \pm 0.15$ ,  $0.13 \pm 0.15$ ,  $0.07 \pm 0.11$ , and  $0.06 \pm 0.11$ ‰). The deepest two samples from station 17 and 18 are 1537 and 1482 m (station 17) and 1509 and 1384 m (station 18), which are within ten or tens of meters to the vent field sea floor (~1542 m).<sup>25,26</sup> The exact distances of each water sample to the vent orifices are unknown. However, previous studies have shown that thermal and chemical anomalies of plumes exhibit peak at 50 m or less from the vent opening, and that buoyant hydrothermal plumes can affect a bottom layer of water up to 100–250 m thick.<sup>26,29,30</sup> A decrease in 650 nm beam transmission was also observed by CTD instrumentation at these bottom depths at station 17 (see the Supporting Information and full CTD data archived at rvddata.us, DOI: 10.7284/907996), indicative of a particle source or nepheloid layer that may be related to a hydrothermal origin—station 17 also exhibited the lowest K isotope ratios at these depths. Nevertheless, the differences between these deepest samples and the global average are at the edge of current analytical precision and thus cannot be entirely resolved from each other with statistical significance. Therefore, we are cautious to make any suggestion that these deepest samples near the ASHES vent field have been influenced by locally advected hydrothermal fluids.

In summary, this study comparing water columns with and without potential hydrothermal inputs does not conclusively show any direct influence on the seawater K isotopic compositions from hydrothermal fluids. Within our current analytical limitations, the modern seawater is homogeneous in terms of K isotopes, which is consistent with the long residence time of K in seawater.<sup>16</sup> So far, there is no peer-reviewed publication available on direct measurements of the K isotope composition of hydrothermal fluids, yet<sup>21</sup> it was assumed to have a very large range from  $-1$  to  $0$ ‰ (cf., seawater  $0.12 \pm 0.07$ ‰) without providing any direct measurements.<sup>9</sup> Here, we observe no direct evidence of hydrothermal influence on seawater K isotope compositions, though we emphasize that our Pacific seawater samples were merely adjacent to a hydrothermal vent system and might not have directly sampled waters with hydrothermal influence. Direct measurements on hydrothermal fluids from the ASHES vents and other vent

systems are required in order to quantify the endmember K isotope compositions of hydrothermal fluids.<sup>21</sup> Further systematic studies of K isotope variations in hydrothermal fluids and their contributions to the seawater K isotope budget need to be conducted.

**4.2. Global Average K Isotope Composition of Seawater.** The global average K concentration of seawater is 399 ppm,<sup>6</sup> and the total ocean mass is about  $1.4 \times 10^{12}$  Tg, thus the total amount of K dissolved in seawater is  $5.6 \times 10^8$  Tg. The annual riverine flux of K is 52–62 Tg,<sup>17–19</sup> while annual hydrothermal flux is 5–36 Tg.<sup>1,5,17–20</sup> Based on the estimation above, the oceanic residence time ( $\tau$ ) of potassium calculated here is 5.7–9.8 million years, which is close to the previously estimated 11 million years.<sup>16</sup> Regardless of which value is used, the residence time of potassium is very long compared to the average mixing time of the oceans, which is about 1000 years. Therefore, potassium is a conservative element in seawater. Potassium and its isotopes are expected to be well mixed among oceans. Accordingly, varying K concentrations measured here correlated with the varying salinity observed across the Atlantic and Pacific samples.

Until recently there were only four individual published analyses of seawater samples (two from the Atlantic ocean and two from the Pacific ocean) in the literature, and their K isotope compositions varied significantly between  $0.03 \pm 0.03$ ,  $0.06 \pm 0.03$ ,  $0.10 \pm 0.07$ , and  $0.14 \pm 0.01$ ‰.<sup>11–14,23</sup> Recently, researchers from the University of Washington<sup>24</sup> conducted the first systematic study on the heterogeneity of K isotopes in seawater, and they defined the ranges of K isotope variations to be  $0.13 \pm 0.04$  to  $0.17 \pm 0.05$ ‰ for the Atlantic ocean,  $0.13 \pm 0.04$  to  $0.15 \pm 0.04$ ‰ for the Pacific ocean, and  $0.12 \pm 0.05$  to  $0.15 \pm 0.04$ ‰ for the Indian ocean. The authors<sup>24</sup> concluded that the K isotopic compositions of global oceans are homogeneous, and the average of all of their samples is  $0.14 \pm 0.02$ ‰.

Our new analyses show results to be consistent with the literature.<sup>24</sup> As seen in Table 1 and Figure 2, all columns show no resolvable variation of K isotopes despite the presence of multiple water masses across depth exhibiting varying temperatures and salinity. The average of K isotope compositions for all samples from this study is  $0.10 \pm 0.08$ ‰, which is indistinguishable from the literature values of  $0.14 \pm 0.02$  and  $0.10 \pm 0.07$ ‰<sup>11,24</sup> but significantly higher than other literature values of  $0.03 \pm 0.03$  and  $0.06 \pm 0.03$ ‰.<sup>12,13</sup>

Combining this study with all literature data,<sup>11–14,23,24</sup> we calculated the most comprehensive average of the modern global seawater constructed from the largest database (70 individual samples from 17 locations in the Atlantic, Pacific, and Indian oceans with varying depths of 0 to 4500 m; see the Supporting Information). We found that there is no resolvable K isotopic difference between the three oceans:  $0.12 \pm 0.08$ ‰ (Atlantic),  $0.11 \pm 0.06$ ‰ (Pacific), and  $0.14 \pm 0.01$ ‰ (Indian). The best available average global K isotope composition of modern seawater calculated here is  $0.12 \pm 0.07$ ‰ (2SD).

This new global average K isotope composition of modern seawater agrees well with the previous reports<sup>11–14,23,24</sup> within analytical uncertainties. It further highlights the large and significant difference between the two major reservoirs on Earth, that is, the ocean and the BSE. A large number of igneous rocks (e.g., ultramafic, mafic, intermediate, and felsic) from different regions and tectonic settings on Earth have been analyzed,<sup>11–15,22,23,31</sup> exhibiting a tight range of K isotopic

variation between  $-0.5$  and  $-0.4\%$ . The BSE values have been defined by multiple groups based on datasets with varying sample sizes, such as  $-0.5$ ,<sup>32</sup>  $-0.48 \pm 0.03$ ,<sup>11</sup>  $-0.52$ ,<sup>33</sup> and  $-0.54 \pm 0.06\%$ .<sup>13</sup> Most recently, the K isotopic compositions of 51 fresh mid-ocean ridge basalts and oceanic island basalts have been analyzed on samples collected from the Atlantic mid-ocean Ridge, East Pacific Rise, Galapagos Ridge, Gulf of Aden, Red Sea, Austral Chain, Hawaii, Society Plume, and North Fiji Basin.<sup>34</sup> The mean value calculated from this largest database of globally distributed fresh oceanic basalts is  $-0.43 \pm 0.17\%$  (2SD), which can be used as the best available representative BSE value. Using this BSE value and the average global K isotope composition of modern seawater in this study, we derived a significant difference of  $0.55 \pm 0.18\%$  between the seawater and BSE.

The reason why seawater is significantly enriched in heavy K isotopes relative to the BSE is still not entirely known and would require quantitatively modeling and balancing the major inputs and outputs of K into seawater, that is, the riverine and hydrothermal inputs as well as the isotopic fractionation during marine sediment formation and reverse weathering.<sup>9</sup> The K isotopic compositions of global riverine inputs, hydrothermal fluids, and isotope fractionation factors during authigenic clay formation and low-temperature alteration have not been well constrained and are still debatable.<sup>3,9,21,22</sup> The well-studied, Li isotope system could become a useful analogue for understanding the global cycling of K isotopes as both Li and K are alkali metals and have similar geochemical behavior. The Li isotope composition of seawater ( $31 \pm 0.05\%$ )<sup>35</sup> has long been known to be enriched in heavy Li isotopes compared to the BSE value ( $3.5\text{--}4.0\%$ ).<sup>36</sup> This heavy Li isotope composition of seawater has been successfully explained by balancing the inputs (from rivers, groundwaters, and hydrothermal fluids) and outputs (through low-temperature alteration of oceanic basalts and authigenic clay formation in sediments).<sup>36</sup> Most importantly, Li isotopes have been used as a tracer of climate change and continental weathering through geological history by applying the same mass-balance box model of Li isotopes of modern seawater into that of the paleo-seawater.<sup>37</sup> It has been found that the Li isotope composition of paleo-seawater was heavier by  $9\%$  during the Cenozoic, which has been linked to the increased riverine flux caused by a stronger continental weathering because of the tectonic uplift.<sup>37</sup> In contrast to Li, K is not a major constituent of carbonates, thus the K isotope flux of riverine inputs to seawater is not affected by carbonate weathering and is mostly dominated by silicate weathering. Thus, combining K isotopes with Li isotopes may better distinguish carbonate weathering from silicate weathering. Similar to Li isotopes, K isotopes have also the potential to become a novel proxy of the secular evolution of continental weathering.<sup>9</sup>

## 5. CONCLUSIONS

In this study, we report the K isotope compositions of 46 seawater samples from four depth profiles from two locations in the Pacific and Atlantic oceans. Seawater samples from both oceans with or without any close affinity to a hydrothermal vent system showed uniform K isotope compositions and no correlation between K isotope composition and location, K concentration, depth, temperature, or salinity. Using these new results, combined with literature data, we calculated the best available average global K isotope composition of modern

seawater to be  $0.12 \pm 0.07\%$  (2SD), which is  $0.55 \pm 0.18\%$  higher than the BSE value.

In addition, we also searched for direct hydrothermal influence on the seawater K isotope composition in seawater samples from above an active hydrothermal vents field (ASHES vent field, Juan de Fuca Ridge) in the Pacific ocean. Considering the current analytical uncertainty, there is no resolvable direct influence from hydrothermal vent systems on the seawater K isotope composition. Nevertheless, direct measurements on hydrothermal fluids are still lacking, and it remains to be investigated what the end-member values of hydrothermal fluids would be, and whether they could significantly change the K isotope budget of the ocean. The hydrothermal inputs to seawater need to be further constrained before applying the K isotope system to understand continental weathering and tracing global K cycling.

## ■ ASSOCIATED CONTENT

### Supporting Information

The Supporting Information is available free of charge at <https://pubs.acs.org/doi/10.1021/acsearthspacechem.0c00047>.

Compilation of K isotope compositions of seawater (individual location), compilation of K isotope compositions of seawater (individual samples), and sample CTD (Conductivity Temperature Depth) data (XLSX)

## ■ AUTHOR INFORMATION

### Corresponding Author

**Kun Wang** – Department of Earth and Planetary Sciences and McDonnell Center for the Space Sciences, Washington University in St. Louis, St. Louis, Missouri 63130, United States; [orcid.org/0000-0003-0691-7058](https://orcid.org/0000-0003-0691-7058); Email: [wangkun@wustl.edu](mailto:wangkun@wustl.edu)

### Authors

**Hilary G. Close** – Rosenstiel School of Marine and Atmospheric Science, University of Miami, Miami, Florida 33149, United States

**Brenna Tuller-Ross** – Department of Earth and Planetary Sciences and McDonnell Center for the Space Sciences, Washington University in St. Louis, St. Louis, Missouri 63130, United States

**Heng Chen** – Department of Earth and Planetary Sciences and McDonnell Center for the Space Sciences, Washington University in St. Louis, St. Louis, Missouri 63130, United States; Lamont-Doherty Earth Observatory, Columbia University, Palisades, New York 10964, United States

Complete contact information is available at:

<https://pubs.acs.org/10.1021/acsearthspacechem.0c00047>

### Notes

The authors declare no competing financial interest.

## ■ ACKNOWLEDGMENTS

We thank Dr. Sumit Chakraborty for the editorial handling and two anonymous reviewers for their constructive comments. We would like to thank Shannon Doherty (Miami) for Pacific sample collection, Dennis Hansell for useful discussions, Chief Scientists Mónica Orellana and Kimberly Popendorf, and captains and crew of R/V Oceanus (OC1808C) and R/V F.G. Walton Smith (WS19110). Cruise activities were funded by

NSF OCE 1634009 (M. Orellana) and the Rosenstiel School of Marine and Atmospheric Science. We thank the McDonnell Center for the Space Sciences for funding our research endeavors.

## REFERENCES

- (1) Bloch, S.; Bischoff, J. L. The Effect of Low-Temperature Alteration of Basalt on the Oceanic Budget of Potassium. *Geology* **1979**, *7*, 193.
- (2) Chan, L.; Edmond, J.; Thompson, G.; Gillis, K. Lithium Isotopic Composition of Submarine Basalts: Implications for the Lithium Cycle in the Oceans. *Earth Planet. Sci. Lett.* **1992**, *108*, 151–160.
- (3) Parendo, C. A.; Jacobsen, S. B.; Wang, K. Isotopes as a Tracer of Seafloor Hydrothermal Alteration. *Proc. Natl. Acad. Sci. U.S.A.* **2017**, *114*, 1827–1831.
- (4) Sun, X.; Higgins, J.; Turchyn, A. V. Diffusive Cation Fluxes in Deep-Sea Sediments and Insight into the Global Geochemical Cycles of Calcium, Magnesium, Sodium and Potassium. *Mar. Geol.* **2016**, *373*, 64–77.
- (5) Staudigel, H. Chemical Fluxes from Hydrothermal Alteration of the Oceanic Crust. *Treatise on Geochemistry*; Elsevier, 2014; pp 583–606.
- (6) Culkin, F.; Cox, R. A. Sodium, Potassium, Magnesium, Calcium and Strontium in Sea Water. *Deep. Res.* **1966**, *13*, 789–804.
- (7) Rudnick, R. L.; Gao, S. *Composition of the Continental Crust of Treatise on Geochemistry*, 2nd ed.; Elsevier Science: Amsterdam, Netherlands, 2014; Volume 4, pp 1–51.
- (8) White, W. M.; Klein, E. M. Composition of the Oceanic Crust. *Treatise on Geochemistry*; Elsevier, 2014; pp 457–496.
- (9) Li, S.; Li, W.; Beard, B. L.; Raymo, M. E.; Wang, X.; Chen, Y.; Chen, J. Isotopes as a Tracer for Continental Weathering and Geological K Cycling. *Proc. Natl. Acad. Sci. U.S.A.* **2019**, *116*, 8740–8745.
- (10) Sun, Y.; Teng, F.-Z.; Hu, Y.; Chen, X.-Y.; Pang, K.-N. Tracing Subducted Oceanic Slabs in the Mantle by Using Potassium Isotopes. *Geochim. Cosmochim. Acta* **2019**, *278*, 353.
- (11) Wang, K.; Jacobsen, S. B. An Estimate of the Bulk Silicate Earth Potassium Isotopic Composition Based on MC-ICPMS Measurements of Basalts. *Geochim. Cosmochim. Acta* **2016**, *178*, 223–232.
- (12) Li, W.; Beard, B. L.; Li, S. Precise Measurement of Stable Potassium Isotope Ratios Using a Single Focusing Collision Cell Multi-Collector ICP-MS. *J. Anal. At. Spectrom.* **2016**, *31*, 1023–1029.
- (13) Morgan, L. E.; Santiago Ramos, D. P.; Davidheiser-Kroll, B.; Faithfull, J.; Lloyd, N. S.; Ellam, R. M.; Higgins, J. A. High-Precision  $^{41}\text{K}/^{39}\text{K}$  Measurements by MC-ICP-MS Indicate Terrestrial Variability of  $\delta^{41}\text{K}$ . *J. Anal. At. Spectrom.* **2018**, *33*, 175–186.
- (14) Hu, Y.; Chen, X.-Y.; Xu, Y.-K.; Teng, F.-Z. High-Precision Analysis of Potassium Isotopes by HR-MC-ICPMS. *Chem. Geol.* **2018**, *493*, 100–108.
- (15) Chen, H.; Tian, Z.; Tuller-Ross, B.; Korotev, R. L.; Wang, K. High-Precision Potassium Isotopic Analysis by MC-ICP-MS: An Inter-Laboratory Comparison and Refined K Atomic Weight. *J. Anal. At. Spectrom.* **2019**, *34*, 160–171.
- (16) Goldberg, E. D. Chemical and Mineralogical Aspects of Deep-Sea Sediments. *Phys. Chem. Earth* **1961**, *4*, 281–302.
- (17) Jarrard, R. D. Subduction Fluxes of Water, Carbon Dioxide, Chlorine, and Potassium. *Geochem., Geophys., Geosyst.* **2003**, *4* (5), No. 8905.
- (18) Holland, H. D. Sea Level, Sediments and the Composition of Seawater. *Am. J. Sci.* **2005**, *305*, 220–239.
- (19) Berner, E. K.; Berner, R. A. *Global Environment: Water, Air, and Geochemical Cycles*; Princeton University Press, 2012.
- (20) Elderfield, H.; Schultz, A. Mid-Ocean Ridge Hydrothermal Fluxes and the Chemical Composition of the Ocean. *Annu. Rev. Earth Planet. Sci.* **1996**, *24*, 191–224.
- (21) Zheng, X.-Y.; Beard, B. L.; Neuman, M.; Fahnstock, M. F.; Bryce, J. G.; Johnson, C. Constraining Stable K Isotope Mass Balance of the Global Ocean and Its Implications for the Modern and Past Silicate Cycle. *Am. Geophys. Union Fall Meet.* **2019**, 2019, No. EP33C.
- (22) Santiago Ramos, D. P.; Morgan, L. E.; Lloyd, N. S.; Higgins, J. A. Reverse Weathering in Marine Sediments and the Geochemical Cycle of Potassium in Seawater: Insights from the K Isotopic Composition ( $^{41}\text{K}/^{39}\text{K}$ ) of Deep-Sea Pore-Fluids. *Geochim. Cosmochim. Acta* **2018**, *236*, 99–120.
- (23) Xu, Y.-K.; Hu, Y.; Chen, X.-Y.; Huang, T.-Y.; Sletten, R. S.; Zhu, D.; Teng, F.-Z. Potassium Isotopic Compositions of International Geological Reference Materials. *Chem. Geol.* **2019**, *513*, 101–107.
- (24) Hille, M.; Hu, Y.; Huang, T.-Y.; Teng, F.-Z. Homogeneous and Heavy Potassium Isotopic Composition of Global Oceans. *Sci. Bull.* **2019**, *64*, 1740.
- (25) Massoth, G. J.; Butterfield, D. A.; Lupton, J. E.; McDuff, R. E.; Lilley, M. D.; Jonasson, I. R. Submarine Venting of Phase-Separated Hydrothermal Fluids at Axial Volcano, Juan de Fuca Ridge. *Nature* **1989**, *340*, 702–705.
- (26) Feely, R. A.; Geiselman, T. L.; Baker, E. T.; Massoth, G. J.; Hammond, S. R. Distribution and Composition of Hydrothermal Plume Particles from the ASHES Vent Field at Axial Volcano, Juan de Fuca Ridge. *J. Geophys. Res.* **1990**, *95*, 12855.
- (27) Kelley, D. S.; Delaney, J. R.; Juniper, S. K. Establishing a New Era of Submarine Volcanic Observatories: Cabling Axial Seamount and the Endeavour Segment of the Juan de Fuca Ridge. *Mar. Geol.* **2014**, *352*, 426–450.
- (28) Strelow, E. W. E.; Toerien, F. V. S.; Weinert, C. H. S. W. Accurate Determination of Traces of Sodium and Potassium in Rocks by Ion Exchange Followed by Atomic Absorption Spectroscopy. *Anal. Chim. Acta* **1970**, *50*, 399–405.
- (29) Lupton, J. E.; Delaney, J. R.; Johnson, H. P.; Tivey, M. K. Entrainment and Vertical Transport of Deep-Ocean Water by Buoyant Hydrothermal Plumes. *Nature* **1985**, *316*, 621–623.
- (30) Baker, E. T.; Massoth, G. J. Hydrothermal Plume Measurements: A Regional Perspective. *Science* **1986**, *234*, 980–982.
- (31) Huang, T.-Y.; Teng, F.-Z.; Rudnick, R. L.; Chen, X.-Y.; Hu, Y.; Liu, Y.-S.; Wu, F.-Y. Heterogeneous Potassium Isotopic Composition of the Upper Continental Crust. *Geochim. Cosmochim. Acta* **2020**, *278*, 122–136.
- (32) Christensen, J. N.; Qin, L.; Brown, S. T.; DePaolo, D. J. Potassium and Calcium Isotopic Fractionation by Plants (Soybean [Glycine Max], Rice [Oryza Sativa], and Wheat [Triticum Aestivum]). *ACS Earth Space Chem.* **2018**, *2*, 745–752.
- (33) Li, W.; Kwon, K. D.; Li, S.; Beard, B. L. Potassium Isotope Fractionation between K-Salts and Saturated Aqueous Solutions at Room Temperature: Laboratory Experiments and Theoretical Calculations. *Geochim. Cosmochim. Acta* **2017**, *214*, 1–13.
- (34) Tuller-Ross, B.; Marty, B.; Chen, H.; Kelley, K. A.; Lee, H.; Wang, K. Potassium Isotope Systematics of Oceanic Basalts. *Geochim. Cosmochim. Acta* **2019**, *259*, 144–154.
- (35) Millot, R.; Guerrot, C.; Vigier, N. Accurate and High-Precision Measurement of Lithium Isotopes in Two Reference Materials by MC-ICP-MS. *Geostand. Geoanal. Res.* **2004**, *28*, 153–159.
- (36) Penniston-Dorland, S.; Liu, X.-M.; Rudnick, R. L. Lithium Isotope Geochemistry. *Rev. Mineral. Geochem.* **2017**, *82*, 165.
- (37) Misra, S.; Froelich, P. N. Lithium Isotope History of Cenozoic Seawater: Changes in Silicate Weathering and Reverse Weathering. *Science* **2012**, *335*, 818–823.